JOURNAL OF VIROLOGY, Dec. 2010, p. 13059–13062 Vol. 84, No. 24
0022-538X/10/$12.00 doi:10.1128/JVI.00912-10

Codon Optimization of Human Parvovirus B19 Capsid Genes Greatly Increases Their Expression in Nonpermissive Cells▽†

Ning Zhi,*‡ Zhihong Wan,‡ Xiaohong Liu, Susan Wong, Dong Joo Kim, Neal S. Young, and Sachiko Kajigaya

Hematology Branch, National Heart, Lung, and Blood Institute, National Institutes of Health, Bethesda, Maryland

Received 28 April 2010/Accepted 4 October 2010

Parvovirus B19 (B19V) is pathogenic for humans and has an extreme tropism for human erythroid progenitors. We report cell type-specific expression of the B19V capsid genes (*VP1* and *VP2*) and greatly increased B19V capsid protein production in nonpermissive cells by codon optimization. Codon usage limitation, rather than promoter type and the 3′ untranslated region of the capsid genes, appears to be a key factor in capsid protein production in nonpermissive cells. Moreover, B19 virus-like particles were successfully generated in nonpermissive cells by transient transfection of a plasmid carrying both codon-optimized *VP1* and *VP2* genes.

Parvovirus B19 (B19V) is a widespread human pathogen that displays a remarkable specificity for erythroid progenitors. There are only a few semipermissive cell lines for B19V, such as UT7/Epo-S1 (8) and KU812Ep6 (7) cells. Recently, we reported that *ex vivo*-generated $CD36^+$ erythroid progenitor cells (EPCs) were highly permissive to B19V infection (10). To date, the preferential B19V propagation in erythroid progenitors is not fully understood. Capsid protein synthesis appears to be restricted to permissive erythroid progenitors, but nonstructural protein 1 (NS1) is produced in both permissive and nonpermissive cells (6, 9). Here, we investigated the expression profile of B19V proteins in permissive and nonpermissive cells and demonstrated that codon optimization significantly improved B19V capsid expression in nonpermissive cells.

To analyze the expression profile of B19V genes, we constructed six plasmids carrying the genes encoding VP1, VP2, NS1, 11-kDa protein, 7.5-kDa protein, and a putative protein X, respectively (11) (Fig. 1A). Each corresponding open reading frame (ORF) was PCR amplified and cloned into a pCMV-3Tag-6 vector (Invitrogen, Carlsbad, CA) to generate Flag-tagged proteins. After transfection of the plasmids into permissive ($CD36^+$ EPC), semipermissive (UT7/Epo-S1), and nonpermissive (293T and HeLa) cells, the levels of protein synthesis were assessed by immunoblotting at 48 h posttransfection (hpt) using anti-Flag M2 antibody (Sigma, St. Louis, MO) (Fig. 1B). VP1 and VP2 expression levels were high in $CD36^+$ EPCs, very low in UT7/Epo-S1 and 293T cells, and undetectable in HeLa cells (Fig. 1B). In contrast, NS1, 11-kDa, 7.5-kDa, and X proteins were produced at high levels in all cells tested.

Codon usage bias has been reported for numerous organisms, from viruses (1) to eukaryotes (5). If a gene contains codons that are rarely used in the host, its expression level will not be maximal. Codon optimization involves altering the rare codons in the target gene so that they more closely reflect the codon usage of the host without modifying the amino acid sequence of the encoded protein. In attempts to improve B19V capsid gene expression, the entire ORF of *VP2* (nucleotides [nt] 3305 to 4969; GenBank nucleotide

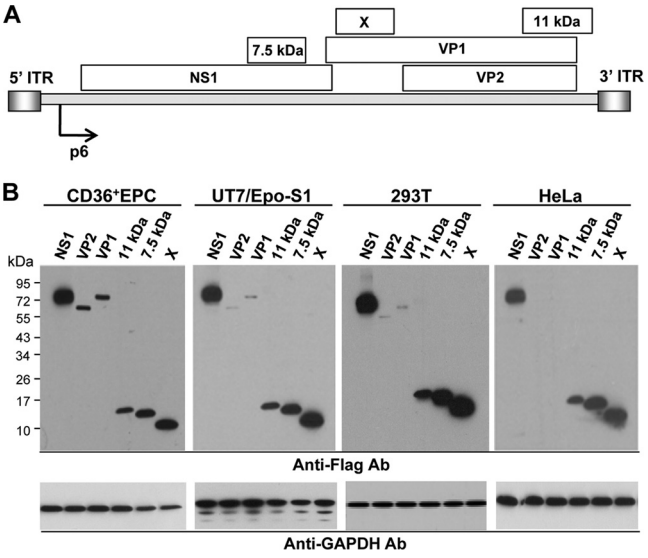

FIG. 1. Cell type-specific expression of B19V capsid proteins. (A) Relevant positions of B19V genes and promoter (p6) in B19V genome. (B) Immunoblotting of B19V capsid protein production in various cells. $CD36^+$ EPCs and UT7/Epo-S1 cells were transfected using the Amaxa Cell Line Nucleofector kit, and 293T and HeLa cells were transfected using Lipofectamine 2000. Whole-cell lysates were prepared at 48 hpt, resolved on 4 to 20% SDS-PAGE gels, and subjected to immunoblotting with anti-Flag antibody. Bands were visualized by using SuperSignal chemiluminescent reagent and then exposure to X-ray film. Numbers on the left indicate the molecular masses (kDa). GAPDH, glyceraldehyde-3-phosphate dehydrogenase.

* Corresponding author. Mailing address: Bldg. 10CRC/Rm. 3E-5272, National Institutes of Health, 9000 Rockville Pike, Bethesda, MD 20892. Phone: (301) 451-7137. Fax: (301) 496-8396. E-mail: zhin@nhlbi.nih.gov.

† Supplemental material for this article may be found at http://jvi.asm.org/.

‡ Ning Zhi and Zhihong Wan contributed equally to this work.

▽ Published ahead of print on 13 October 2010.

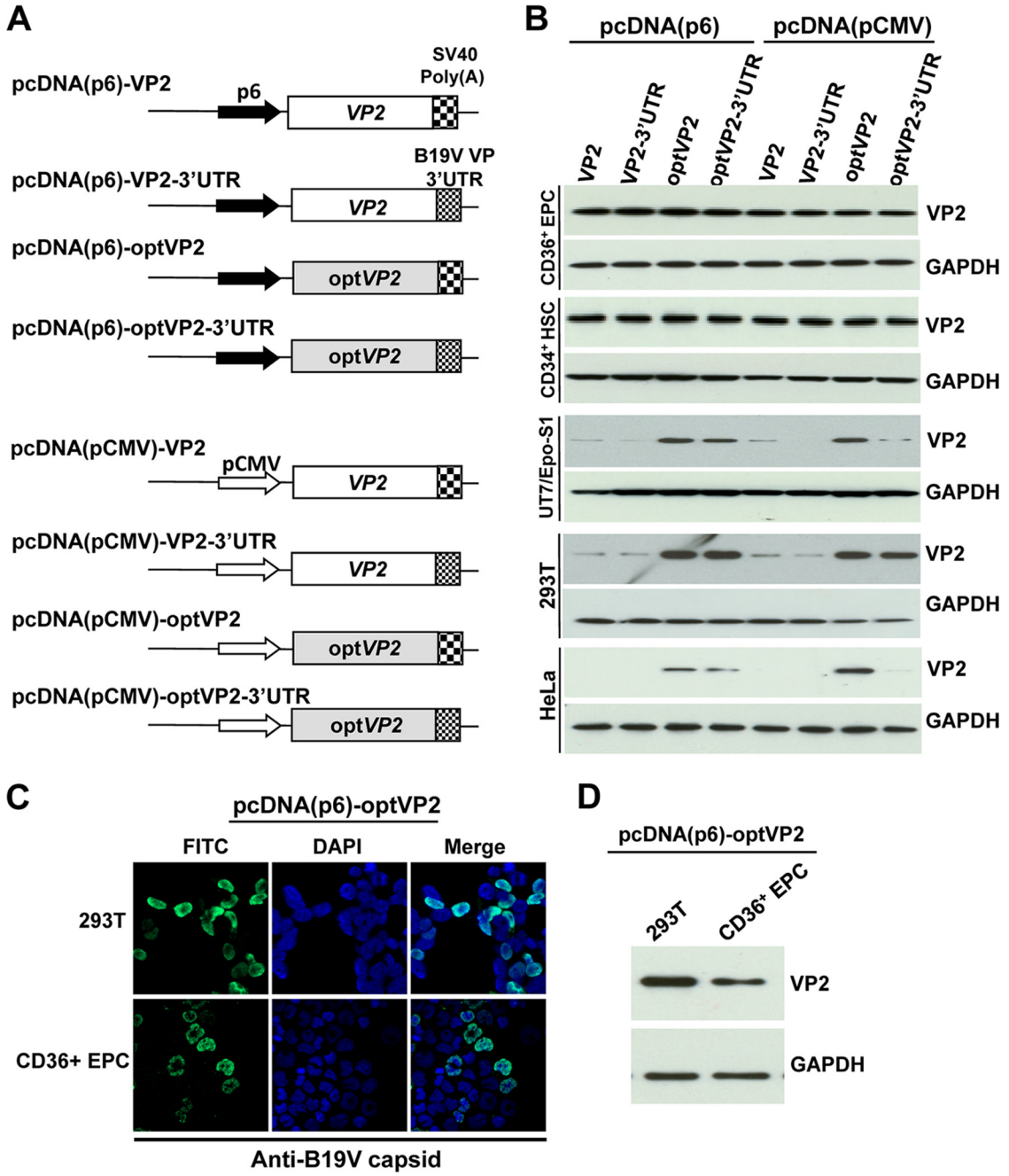

FIG. 2. Codon usage is critical for B19V capsid protein production. (A) Schematic diagram of plasmid construction. (B) Immunoblotting of VP2 production in $CD36^+$ EPCs, $CD34^+$ HSCs, and three different cell lines. Following transfection with individual plasmids, whole-cell lysates were prepared at 48 hpt and subjected to 4 to 20% SDS-PAGE, followed by immunoblotting with anti-VP2 antibody (MAb 8293). (C) IF assay. Cells transfected with pcDNA(p6)-optVP2 were immunostained with anti-VP2 antibody (MAb 8292) specific for a conformational epitope and then fluorescein isothiocyanate (FITC)-conjugated secondary antibody (green), followed by 4′,6-diamidino-2-phenylindole (DAPI) nuclear counterstaining. (D) Immunoblotting. 293T cells and $CD36^+$ EPCs were transfected with pcDNA(p6)-optVP2 and subjected to immunoblotting with the anti-VP2 antibody (MAb 8293).

sequence accession no. AY386330) was codon optimized for better expression in mammalian cells and synthesized by Celtek Bioscience, LLC (Nashville, TN) (see Fig. S1 in the supplemental material). To further elucidate *cis* elements that may influence the expression of *VP2*, we constructed eight plasmids using codon-optimized *VP2* (*optVP2*) and wild-type *VP2* (*VP2*). Briefly, *VP2* or *optVP2* genes with or without the 3′ untranslated region (UTR) (nt 4970 to 5409) of the B19V *VP2* gene were inserted into a pcDNA(p6) vector in which a cytomegalovirus (CMV) promoter of pcDNA3.1 (Invitrogen) was replaced with a B19V p6 promoter (p6, nt 188 to 584) (Fig. 2A). Likewise, *VP2* or *optVP2*

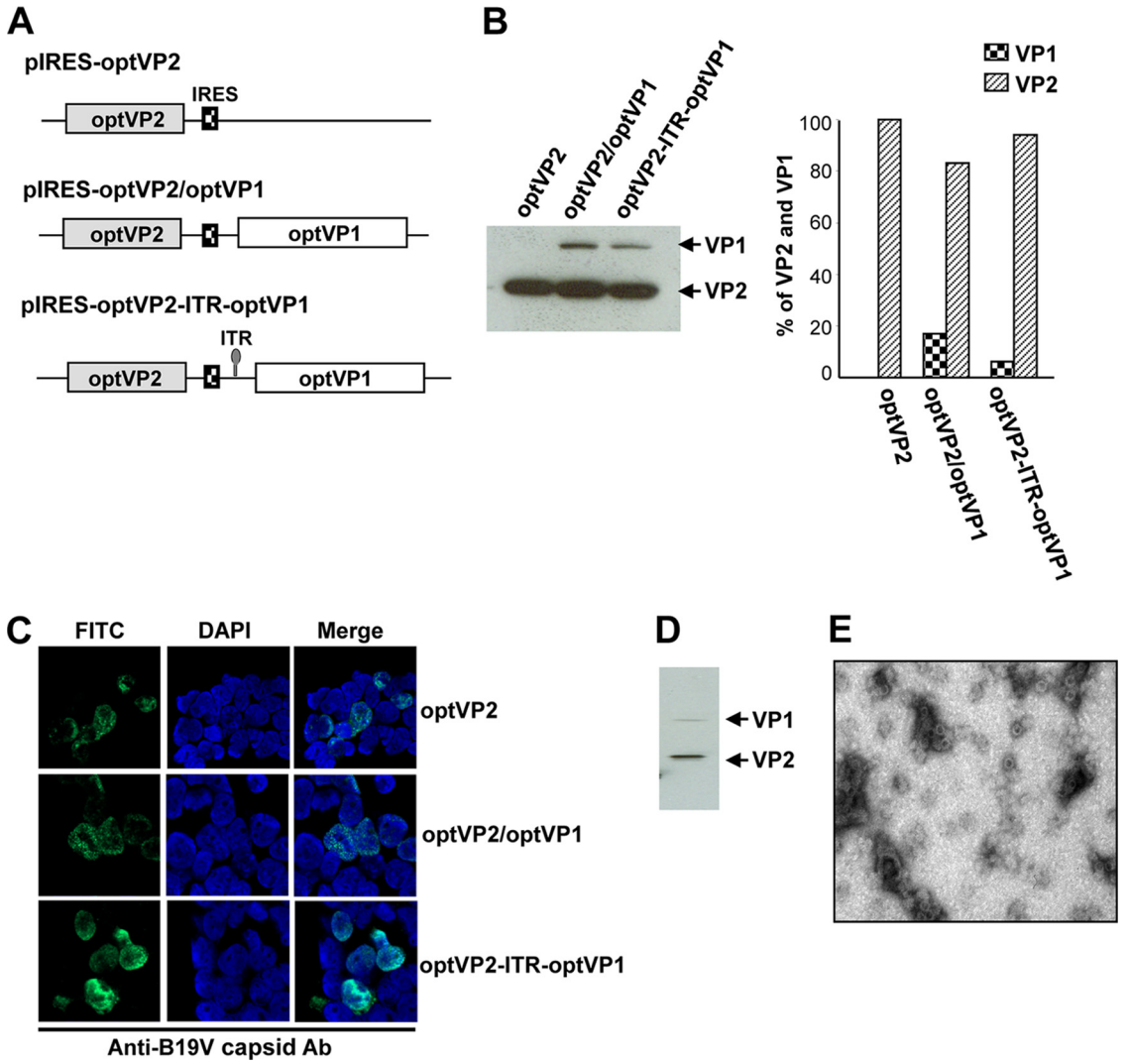

FIG. 3. Production of B19V VLPs in nonpermissive cells after codon optimization. (A) Schematic diagram of plasmid construction. IRES, internal ribosome entry site. (B) Immunoblotting of B19V capsid proteins in 293T cells. After transfection of individual plasmids into the cells, whole-cell lysates were subjected to 4 to 20% SDS-PAGE and subsequently immunoblotting with anti-VP2 antibody (MAb 8293). (C) Transfected cells were immunostained with anti-VP2 antibody (MAb 8292) and then FITC-conjugated secondary antibody (green). (D) Immunoblotting of the pellet after ultracentrifugation with anti-VP2 antibody (MAb 8293). (E) Cells transfected with pIRES-optVP2-ITR-optVP1 were lysed and clarified by low-speed centrifugation, followed by ultracentrifugation by loading on 40% sucrose. Pellet was resuspended and analyzed by transmission electron microscopy after negative staining. Magnification, ×154,000.

with or without the 3′ UTR was inserted into pcDNA3.1 in which expression of the B19V capsid gene was controlled by the CMV promoter (pCMV) (Fig. 2A). Using these plasmids, expression levels of *VP2* were evaluated in different cells by immunoblotting with anti-VP2 antibody (monoclonal antibody [MAb] 8293; Chemicon, Temecula, CA) (11). At 48 hpt, $CD36^+$ EPCs and $CD34^+$ hematopoietic stem cells (HSCs) produced high levels of VP2 protein (Fig. 2B) regardless of codon usage (*VP2* or *optVP2*), promoter type (p6 or pCMV), or 3′ UTR type (B19V *VP2* 3′ UTR or simian virus 40 [SV40] early polyadenylation sequence). Interestingly, although a previous study showed that $CD34^+$ HSCs were not permissive for B19 infection (10), VP2 was produced in $CD34^+$ HSCs at levels similar to those in $CD36^+$ EPCs. To assess *VP2* expression in $CD36^+$ EPCs and 293T cells, cells were transfected with pcDNA(p6)-optVP2 and subjected to immunofluorescence (IF) assay and immunoblotting. As shown in Fig. 2C and D, *optVP2* expression in 293T cells and that in $CD36^+$ EPCs were comparable, indicating that VP2 production was dramatically enhanced by codon optimization. A similar enhancement has been reported for various genes in a variety of viruses, including human herpesvirus (2), papillomavirus (3), hepatitis A virus (1), and hepatitis C virus (4). We observed a decreased VP2 production when the plasmids carrying *VP2* or *optVP2* with B19V 3′ UTR were utilized. This B19V 3′-UTR-related inhibition of VP2 production was particularly apparent in UT7/Epo-S1 and HeLa cells but not obvious in 293T cells, $CD34^+$ HSCs, and $CD36^+$ EPCs. Additionally, B19V 3′-UTR-related inhibition appeared to

be greater in the context of the pCMV-controlled transcription than in that of p6-controlled transcription. This finding suggests that the negative impact of B19V 3′ UTR on capsid production was promoter and cell type dependent.

To generate empty B19V virus-like particles (VLPs) composed of *optVP1* and *optVP2*, a B19V *optVP1* gene was synthesized in the same manner as that described for *optVP2*. Both *optVP1* and *optVP2* were subcloned into a pIRES bicistronic expression vector (Clonetech), resulting in pIRES-optVP2/optVP1. To adjust the VP1/VP2 ratio, an inverted repeat (ITR, 5′-GGATCCCGACGATCC-3′) sequence was inserted immediately upstream of *optVP1* (Fig. 3A). When 293T cells were transfected with individual plasmids, overall VP2 production levels were similar among the three samples (Fig. 3B). The VP1/VP2 ratio was 1:5 or 1:20 in the cells transfected with pIRES-optVP2/optVP1 or pIRES-optVP2-ITR-optVP1, respectively, showing that the VP1/VP2 (1:20) ratio of the natural B19V capsid was obtained by the ITR insertion. By IF assay, B19V capsid proteins were detected predominantly in nuclei at 24 hpt (Fig. 3C). Next, we attempted to generate B19V VLPs in 293T cells using pIRES-optVP2-ITR-optVP1, by which the natural VP1/VP2 ratio was obtained. When cell lysates were subjected to sequential sedimentation in sucrose and CsCl, banding of parvovirus proteins was detected at 1.31 g/ml (density of empty capsid), and VP1 and VP2 were detected by immunoblotting (Fig. 3D). Direct electron microscopy of the sample revealed typical parvovirus-like particles (Fig. 3E).

In summary, we demonstrate cell type-specific expression of B19V capsid proteins and a dramatic increase in capsid protein production in nonpermissive cells by codon optimization. Using the *optVP1* and *optVP2* genes, empty B19V VLPs were generated in 293T cells. Although further studies are required for optimal production of B19V VLPs, our current work provides new insight for B19V research using nonpermissive cells and may be of practical importance in vaccine development.

We thank Daniela Malide, Light Microscopy Core Facility, NHLBI for assistance with confocal microscopy.

This study was supported by the Intramural Research Program of the NIH, NHLBI.

REFERENCES

1. **Aragones, L., S. Guix, E. Ribes, A. Bosch, and R. M. Pinto.** 2010. Fine-tuning translation kinetics selection as the driving force of codon usage bias in the hepatitis A virus capsid. PLoS Pathog. **6:**e1000797.
2. **Bradel-Tretheway, B. G., Z. Zhen, and S. Dewhurst.** 2003. Effects of codon-optimization on protein expression by the human herpesvirus 6 and 7 U51 open reading frame. J. Virol. Methods **111:**145–156.
3. **Cheung, Y. K., S. C. Cheng, F. W. Sin, and Y. Xie.** 2004. Plasmid encoding papillomavirus type 16 (HPV16) DNA constructed with codon optimization improved the immunogenicity against HPV infection. Vaccine **23:**629–638.
4. **Frelin, L., G. Ahlen, M. Alheim, O. Weiland, C. Barnfield, P. Liljestrom, and M. Sallberg.** 2004. Codon optimization and mRNA amplification effectively enhances the immunogenicity of the hepatitis C virus nonstructural 3/4A gene. Gene Ther. **11:**522–533.
5. **Grantham, R., C. Gautier, and M. Gouy.** 1980. Codon frequencies in 119 individual genes confirm consistent choices of degenerate bases according to genome type. Nucleic Acids Res. **8:**1893–1912.
6. **Liu, J. M., S. W. Green, T. Shimada, and N. S. Young.** 1992. A block in full-length transcript maturation in cells nonpermissive for B19 parvovirus. J. Virol. **66:**4686–4692.
7. **Miyagawa, E., T. Yoshida, H. Takahashi, K. Yamaguchi, T. Nagano, Y. Kiriyama, K. Okochi, and H. Sato.** 1999. Infection of the erythroid cell line, KU812Ep6 with human parvovirus B19 and its application to titration of B19 infectivity. J. Virol. Methods **83:**45–54.
8. **Morita, E., K. Tada, H. Chisaka, H. Asao, H. Sato, N. Yaegashi, and K. Sugamura.** 2001. Human parvovirus B19 induces cell cycle arrest at G(2) phase with accumulation of mitotic cyclins. J. Virol. **75:**7555–7563.
9. **Pallier, C., A. Greco, J. Le Junter, A. Saib, I. Vassias, and F. Morinet.** 1997. The 3′ untranslated region of the B19 parvovirus capsid protein mRNAs inhibits its own mRNA translation in nonpermissive cells. J. Virol. **71:**9482–9489.
10. **Wong, S., N. Zhi, C. Filippone, K. Keyvanfar, S. Kajigaya, K. E. Brown, and N. S. Young.** 2008. Ex vivo-generated CD36+ erythroid progenitors are highly permissive to human parvovirus B19 replication. J. Virol. **82:**2470–2476.
11. **Zhi, N., I. P. Mills, J. Lu, S. Wong, C. Filippone, and K. E. Brown.** 2006. Molecular and functional analyses of a human parvovirus B19 infectious clone demonstrates essential roles for NS1, VP1, and the 11-kilodalton protein in virus replication and infectivity. J. Virol. **80:**5941–5950.